

Application of the CFAST Zone Model to Ships – Fire Specification Parameters

JOHN B. HOOVER*

*Chemistry Division, US Naval Research Laboratory
Washington, DC 20375 USA*

ABSTRACT: An analysis of the sensitivity of the Consolidated Fire and Smoke Transport model to several key fire specification parameters has been performed for this paper. Results of simulations of shipboard fires are compared with data from full-scale experiments. It was found that reasonable estimates of the fire inputs, with the exception of the smoke and carbon monoxide production parameters, could be obtained from literature values. The soot parameter was found to be critical for accurate temperature predictions, especially in the upper layer.

KEY WORDS: fire model, zone model, CFAST, model validation, model inputs.

INTRODUCTION

THE CONSOLIDATED FIRE and Smoke Transport (CFAST) model was developed at the National Institute of Standards and Technology (NIST) as a tool for predicting the effects of fires in buildings [1]. It is a multi-compartment zone model and, as in most such models, the atmosphere in each room is represented as two homogeneous layers (zones) separated by a dynamic horizontal interface. Walls are divided into upper and lower regions corresponding to the instantaneous position of the interface. Each zone is then bounded by a single wall (which wraps around all four sides), one horizontal surface (floor or ceiling, as appropriate) and the zone interface. Conditions in each zone and in the ceiling, floor and wall boundaries are predicted by solving a set of time-dependent, ordinary differential equations.

In order to ensure reasonable performance on the computer hardware available at the time, the CFAST developers made simplifications in

*E-mail: john.hoover@nrl.navy.mil

several key areas. For example, complex geometries were replaced by simple, rectilinear parallelepipeds; correlation functions, rather than *ab initio* equations, were used for some phenomena (e.g., plumes); and some phenomena were completely neglected. Arguably, the most important of the neglected phenomena was the fire itself [2]. Rather than attempt to predict fire growth using a self-consistent fire growth model, the developers chose to require a user-provided fire specification that defines heat release rate (HRR), combustion product ratios and other key fire parameters [3] as functions of time.

Other than those related to location, these fire parameters may be placed into three categories depending on whether they reflect fuel, pyrolysis or combustion properties. Fuel parameters, which include chemical composition and heat of combustion, may be specified if the fuel is well characterized but, in practice, real fuels often are not. Pyrolysis and combustion properties are dependent on instantaneous conditions and cannot be known in advance. Due to these uncertainties, development of a meaningful fire description is one of the most difficult aspects of applying CFAST.

The assumptions that underlie the CFAST algorithms impose some limitations on the range of scenarios that can be modeled and on the accuracy of the resulting predictions. However, in many cases of practical interest, the restrictions have not been unduly onerous. CFAST has been successfully used to simulate many building-related fire protection problems. Typical examples include the application to several single- and multi-room fires [1], an entire six-room, single-floor house [4], a multistory, multi-room building [5], several types of atria [6], and a high-aspect airport terminal [7].

In principle, CFAST should also be applicable to shipboard fire problems. However, in some ways, fires aboard ships behave differently from fires in buildings due to the unique environment. For example, ships and buildings differ significantly in materials, construction methods, passive ventilation and fuel loads. The use of thin, highly conductive materials makes conduction a much more important phenomenon than is typically the case in buildings. Ships, unlike buildings, usually have many hatches and scuttles that permit vertical, bidirectional vent flows between compartments on adjacent decks. Finally, a high percentage of the fuel load on ships is composed of flammable liquids, especially petroleum products, rather than wood, wall board or similar structural materials.

As a result of these differences, accurate simulations of shipboard fires required the addition of capabilities for modeling phenomena that are absent from, or of little significance to, building fires. Over a period of years, the US Navy funded efforts to add these features to CFAST. In particular, vertical heat transport via conduction through decks [8], an improved radiation transport sub-model [9], and algorithms for long, narrow passageways [10]

have been added to CFAST specifically to support modeling of shipboard fires. More recently, the wall heat conduction algorithms have been modified to better account for conduction through bulkheads and, as of version 6, CFAST has been converted to a Windows® application¹. Note that, as a result of the latter change, the organization and format of the input files has been drastically altered so that previous input files are no longer usable. The CEdit program, which organizes and displays information from multiple input files, is the primary interface to CFAST.

The current work builds on earlier work using CFAST version 3.1.4 [11]. The primary motivations were to evaluate the capabilities of the CFAST improvements in the context of shipboard fires, to investigate the impact of the inevitable uncertainties in the fire specification and to identify issues requiring further research. In order to address these issues, a full-scale fire conducted aboard the US Navy's test ship ex-USS Shadwell was modeled.

EXPERIMENTS

As part of a program to investigate shipboard ventilation issues, NRL conducted a series of more than 100 tests aboard the ex-USS Shadwell during January 1996. The test area, shown in Figure 1, was located in the Shadwell port wing wall. Test 4–10 was selected for this case study for two reasons: the fire was located in the laundry room and the ventilation ducts were physically blocked. As the only rectangular compartment in the test area, the laundry room provided a geometrically simple starting point for developing the model. The blockage of the ducts made it unnecessary to model the complex ventilation system and greatly simplified the problem. Details of the test program are given in [12] and will only be summarized here.

The laundry room was constructed of steel of several different thicknesses. The overhead, deck, and forward bulkhead thickness was 9.5 mm (0.375 in.), the aft and port bulkhead thickness was 3.2 mm (0.125 in.) and the starboard bulkhead thickness was 12.7 mm (0.500 in.). The door to the laundry passageway provided the only ventilation, although there were undoubtedly small, unquantified leaks at some of the welds due to fire damage from previous tests.

As shown in Figure 2, the fire was a 1.06 m (4 ft) diameter pool of marine diesel fuel, located in front of the door at 1.8 m (W) × 0.84 m (D) (6.0 ft × 2.8 ft). The fire pan was supported, at an elevation of 0.19 m (0.62 ft), by a load cell that provided the mass loss data used in the fire

¹Prior versions were Unix- or DOS-based command line tools.

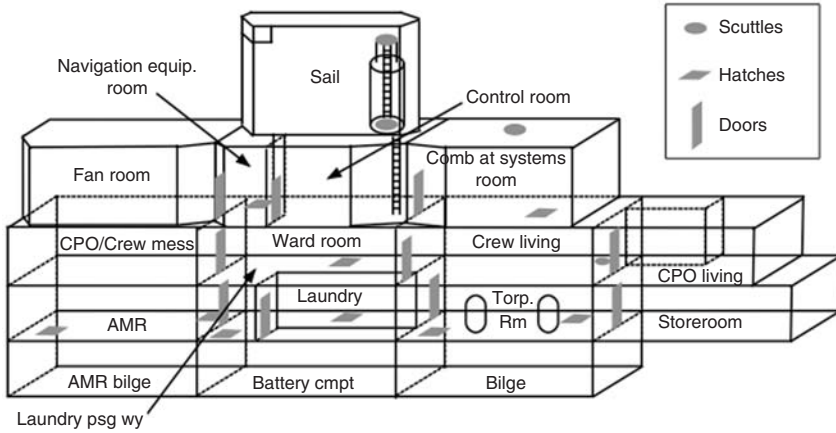


Figure 1. Configuration of the Shadwell port wing wall test area: the fires modeled during this study were diesel pan fires, located in the laundry room.

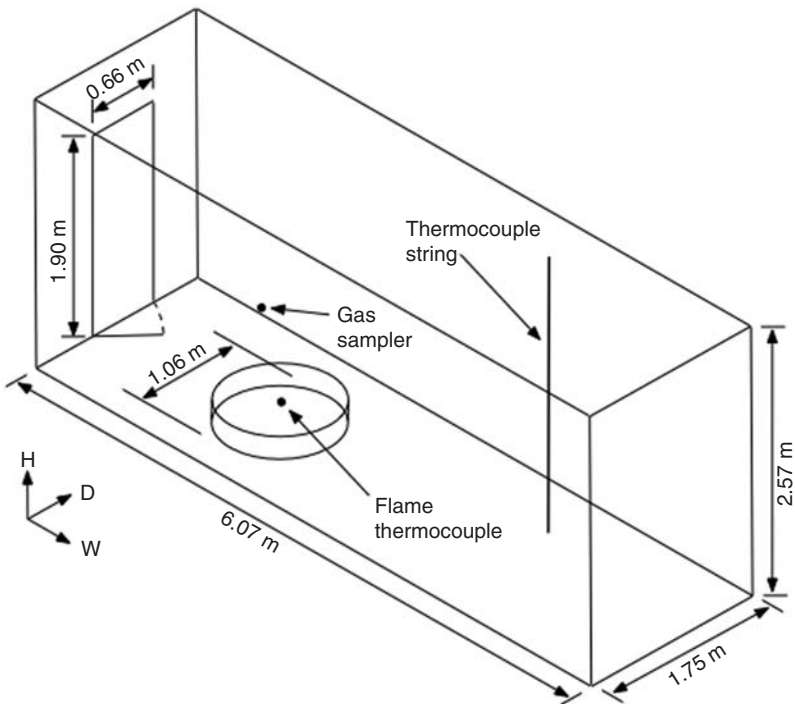


Figure 2. Laundry room dimensions: configuration of the laundry room, with the fire pan centered at $1.83\text{ m (W)} \times 0.91\text{ m (D)} \times 0.19\text{ m (H)}$. The locations of the thermocouple string, flame thermocouple and gas sampling intakes are indicated. The origin of the coordinate system is the lower, left, front corner of the compartment.

definition, as discussed below. A vertical array of thermocouples, at elevations of 0.14, 0.50, 0.95, 1.27, 1.94, and 2.50 m (0.46, 1.6, 3.1, 4.2, 6.36, and 8.20 ft) above the deck, was located forward of the fire pan at 4.32 m (W) \times 1.28 m (D) (14.2 ft \times 4.20 ft). An additional thermocouple, directly above the fire pan, provided flame temperatures and confirmed ignition of the fire. A gas intake for oxygen, carbon dioxide and carbon monoxide analyzers was also located near the fire at 1.19 m (W) \times 1.26 m (D) \times 0.56 m (H) (3.90 ft \times 4.13 ft \times 1.84 ft). Data were collected at one second intervals by custom data acquisition hardware and software.

MODELING

Because the purpose of the current work was to investigate issues related to the fire specification, the complications introduced by complex geometry were to be avoided. Therefore, only the compartment of origin, which had a simple, rectilinear geometry, was modeled. Of greatest interest was the prediction of the compartment temperatures; predictions of species concentrations were of lesser importance. This emphasis was largely motivated by the dearth of species data, combined with the location of the available species data – the intake was located very close to the fire, and therefore the results were probably not representative of the average concentrations within the entire compartment.

Simulations were performed with CFAST version 6.0.7, which was the current version at the time this work started. In developing the model, the approach was to set as many of the inputs as possible to ‘real’ values, i.e., values which are known (or believed, with some justification) to apply to the situation being simulated. In the case of inputs for which there were no specific *a priori* values, values were varied over reasonable ranges in order to investigate the sensitivity to those inputs. With the exception of data relevant to the definition of initial conditions and fuel mass loss rate, no experimental data were used during development of the model inputs.

Model inputs were specified in three files. The main input file (Laundry_Fire.in) defines the compartment geometry and simulation control parameters while the fire object file (Laundry_Fire.o) includes parameters specific to a particular fire. In addition, several materials were added to the default thermophysical database file (thermal.csv). Further details of the syntax and semantics of these files may be found in Peacock et al. [13] and Jones et al. [14].

The simulation control, ambient environment and most of the compartment geometry inputs (Table 1) were trivial. In test 4–10, the fire began to decay at about 1200 seconds so the simulation time was set to 1250 seconds. The screen output interval was set to 1 second while the output intervals for

Table 1. Simulation input file.

```

VERSN,6,Shadwell/688 Laundry Cmpt
!!Environmental keywords
TIMES,1250,1,3,3,3
EAMB,286.3,101300,0
TAMB,285.9,101300,0,100
LIMO2,10
WIND,0,0,0,0.16
CJET,OFF
!!Compartment keywords
COMPA,Laundry,6.07,1.75,2.57,0,0,0,SHIP3/8,SHIP3/8,SHIPLR
!!Vent keywords
HVENT,1,2,1,0.66,1.9,0,1,0,0,1,1
!!Fire keywords
OBJECT,Laundry_Fire,1,1.83,0.84,0.19,1,1,0,0,0,1

```

history, SmokeView² and spreadsheet files were 3 seconds. Experimental values were used for the exterior and interior temperatures (286.3 and 285.9 K, respectively); pressures were assumed to be 101.3 kPa (one standard atmosphere) and the compartment deck elevation was set to zero, the same elevation as the internal and external ambient reference points. Relative humidity is not a critical parameter (it is only used to initialize the water vapor mass loading) and, since tests were performed in a high-humidity shipboard environment, this input was set to 100%.

The main input file also contains three parameters, LIM02, WIND, and CJET, which require some explanation. LIM02, the lower oxygen limit, is the oxygen mass fraction below which CFAST ‘turns off’³ combustion. Because this fire was not ventilation limited, LIM02 was not important and was left at the default value of 0.10. The three parameters associated with the WIND keyword specify the wind velocity, reference elevation and lapse rate coefficient for extrapolating to other elevations. Since the tests were conducted within the confines of a ship, the wind velocity was set to 0 m/second at an elevation of 0 m and the default lapse coefficient (0.16) was used. CJET is a global parameter that invokes different algorithms to describe heat transfer between a plume and the surfaces with which it comes into contact. For this study, the jet was initially turned off but, after the fire description was fully developed, a comparison among all possible values was conducted.

Compartment dimensions were taken from Figure 2 and two materials (SHIP3/8 for the overhead and deck; SHIPLR for the bulkhead) were specified in the CFAST materials database (see below).

²SmokeView is a utility program that displays animations of the simulations.

³CFAST uses a hyperbolic function to produce a smooth but rather sharp transition from normal burning to no combustion [14].

Table 2. Time-independent fire parameters.

Parameter	Value
Fire object name	Laundry_Fire
Number of points	2
Molecular weight (kg/mol)	0.184
Gaseous ignition temperature (K)	330.0
Volatilization temperature (K)	285.9
Heat of gasification (J/kg)	258000
Radiative fraction	0.3
Total mass (kg)	62.4
Length (m)	0.91
Width (m)	0.91
Thickness (m)	0.1
Heat of combustion (J/kg)	4.19E+07
Fuel name	MARINE_DIESEL

The door leading to the laundry passageway was defined as horizontal vent number one connecting compartments one (laundry room) and two (the exterior), having a width of 0.66 m (2.16 ft), a soffit height of 1.90 m (6.23 ft) and a sill height of zero. The vent closure parameter was set to 1.0 (fully open) for the entire simulation. The fire was defined to be a Laundry_Fire object located at 1.83 m (W) \times 0.84 m (D) \times 0.19 m (H) (6.00 ft \times 2.76 ft \times 0.62 ft), having a horizontal burning surface (vertical normal vector) and igniting at 0 seconds.

Time-independent fire properties are given in Table 2, which shows the first entry in each row of the fire object specification file. The “number of points” parameter refers to the number of times used to specify time-dependent parameters, as discussed below. Since the exact composition of the diesel fuel was not known, fuel properties were estimated from literature sources. The molecular weight and heat of combustion for typical marine diesel fuels were taken from [15] and the vapor ignition temperature was based on the minimum flash point for number two diesel fuel, which is specified by ASTM [16] as 52°C (325 K). Because refiners provide a safety margin above this minimum requirement, it was assumed that the actual ignition temperature would be 10 percent higher, or 57°C (330 K). The volatilization temperature was assumed to be the ambient temperature (the default value) while the heat of gasification was estimated by extrapolating the heats of vaporization of C₆–C₁₀ hydrocarbons to dodecane (C₁₂) [17], which was used as a surrogate for diesel fuel. The 0.91 m \times 0.91 m (2.98 ft \times 2.98 ft) dimensions for the fire were based on a square having an area equivalent to that of the actual (circular) pan. The depth of the fire pan was used as the fuel thickness and the mass of fuel was calculated from the fuel volume.

Table 3. Time-dependent fire parameter values.

Time (s)	dQ/dt (W)	dM/dt (kg/s)	Height (m)	Area (m)	O ₂	HCR	CO	OD	HCN	HCl	Ct
0	1060070	0.0253	0	0	0	0.143	0	0	0	0	0
1250	959510	0.0229	0	0	0	0.143	0	0	0	0	0

Radiative fraction (RF) represents the fraction of thermal energy that is radiated from the fire, the remainder being convected via the fire plume. For real fires, the radiative fraction is related to the amount of soot produced. However, in CFAST, radiative fraction and soot production are controlled by independent inputs. The default RF value, 0.3, is believed to be a reasonable value for sooty fires. Since CFAST does not calculate instantaneous combustion conditions, radiation transport effects are only coarse approximations regardless of the accuracy of this input. Simulations were run using RF values ranging from 0.15 to 0.50.

CFAST provides a mechanism by which the user may specify values for several time-dependent fire parameters. The object fire specification provides parameter values for defined times, as shown in Table 3; the model calculates intermediate values by linear interpolation. The 'number of points' parameter from column one specifies the number of rows used to define time-dependent values.

The most important of these variable parameters are the fuel mass loss rate (dM/dt) and heat release rate (dQ/dt). Given either one, CFAST calculates the other using the heat of combustion of the fuel. In addition to these two, the height and area of the base of the fire, the amount of oxidizer incorporated into the fuel, and parameters governing several product production rates may be given.

Because the goal of this work was to determine how well CFAST simulated a specific test fire, it was very important that the fire description accurately represent the actual fire. Therefore, data from the test were used to estimate the mass loss rate inputs. The smoothed (five-point sliding average) fuel mass data were fitted with both linear and exponential curves; the latter was found to be a better fit and was used to estimate the mass loss rate as a function of time, as illustrated in Figure 3. Since the mass loss rate curve was nearly linear, only the initial and final fuel consumption rates (0.0253 and 0.0229 kg/s, respectively) were specified, as shown in Table 3, and CFAST performed an implicit linear interpolation for intermediate times.

Height, the elevation of the burning surface above that specified in the main input file, was set to zero since the pool elevation was essentially constant. The fire area parameter is used only for flame height estimates and does not affect the heat release rate. Diesel fuels have no included oxidizing

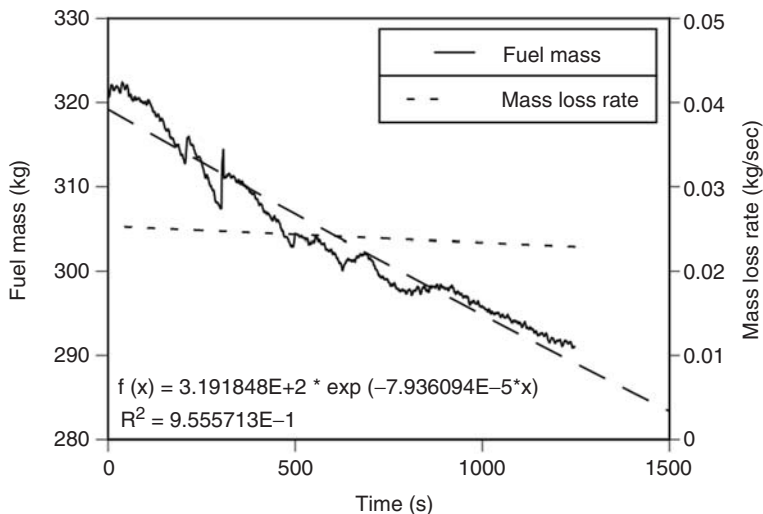


Figure 3. Fuel mass and mass loss rate: as described in the text, an exponential curve (long dashes) was fitted to the smoothed fuel mass data (solid curve, left axis) and the-fitting parameters were then used to calculate the mass loss rate (short dashes, right axis).

agent, so the oxygen-carbon ratio (O_2^4 keyword) was zero. It was assumed that there were negligible amounts of nitrogen and chlorine compounds in the fuel, which allowed the HCN and HCl ratios to be set to zero. Ct is a fictitious ‘species,’ which may be used to estimate overall toxicity. It was not of interest in this work and was therefore defined to be zero.

The parameters OD and CO specify the soot-carbon dioxide and carbon monoxide-carbon dioxide mass ratios, respectively, in the combustion products. In actual fires, both of these ratios vary in complex ways in response to changes in combustion conditions. Since there is no *a priori* way of knowing what those conditions will be, it is not possible to specify OD or CO with certainty. Accordingly, the sensitivity of CFAST to a range of values was investigated, as described subsequently.

The remaining parameter is ‘HCR’ (the hydrogen-carbon ratio in the fuel), which was estimated from the minimum hydrogen content, 12.5% by weight, given by the fuel specification [18]. Assuming a pure hydrocarbon, the following results:

$$184 \text{ g fuel/mole fuel} \times 0.125 = 23 \text{ g H/mole fuel} \quad (1)$$

$$(184 \text{ g fuel/mole fuel}) - (23 \text{ g H/mole fuel}) = (161 \text{ g C/mole fuel}) \quad (2)$$

⁴In common usage, O_2 , HCN, HCl, and CO refer to species and OD to optical density. However, in this article, they are always used in the CFAST context, in which they are keywords, and species names are spelled out.

Table 4. Materials added to the thermophysical properties database.

Short name	Cond. (W/m K)	C _p (J/kg m)	Density (kg/m ³)	Thick. (m)	Emiss.	HCI	Long name
MARINE_DIESEL	0.126	2106	750	0.1	0.04	0	Marine diesel fuel
SHIP3/8	48	559	7854	0.0095	1	0	Carbon steel (0.375 in.)
SHIPLR	48	559	7854	0.0076	1	0	Carbon steel (0.298 in.)

and HCR is

$$(23 \text{ g H/mole fuel})/(161 \text{ g C/mole fuel}) = 0.143 \quad (3)$$

The additions to the thermophysical data are shown in Table 4. Heat capacity and thermal conductivity for the fuel (MARINE_DIESEL) were estimated from Clarke [17] and SAE [19], respectively, the density of dodecane was used, fuel thickness was the depth of the fire pan and emissivity was set to a value typical of a low-absorbance material.

The entries for structural materials (SHIP3/8 and SHIPLR) were based on the standard entry for sheet steel but, since the compartment surfaces were heavily sooted, the surface emissivities for both were set to 1.0 rather than to the default value (0.9) that is more typical of clean steel. The parameter, SHIP3/8, was defined to be 9.5 mm (0.375 in.) thick. CFAST does not permit the use of multiple thicknesses for any single boundary, so the thickness of SHIPLR, 7.6 mm (0.298 in.), was calculated as the area-weighted mean of the actual bulkhead thicknesses.

Sensitivity to OD and CO Parameters

For flaming fires, the carbon monoxide to carbon dioxide mass ratio (CO parameter) is expected to be in the range 0.001–0.02 [20]; values were selected from zero to 0.10, the latter representing an extreme case. For soot production (OD parameter), the upper limit was set to 0.10 and the lower to zero. This was intended to span the range from perfectly clean to extremely sooty fires.

Figure 4(a) shows the effects on the upper layer gas temperature due to variations in OD and CO. The most critical factor is the presence or absence of soot. Given the presence of some soot, the temperature is much lower than in the soot-free case but, beyond that, the temperature has only a small, inverse dependence on the soot parameter. In the lower gas layer, shown in

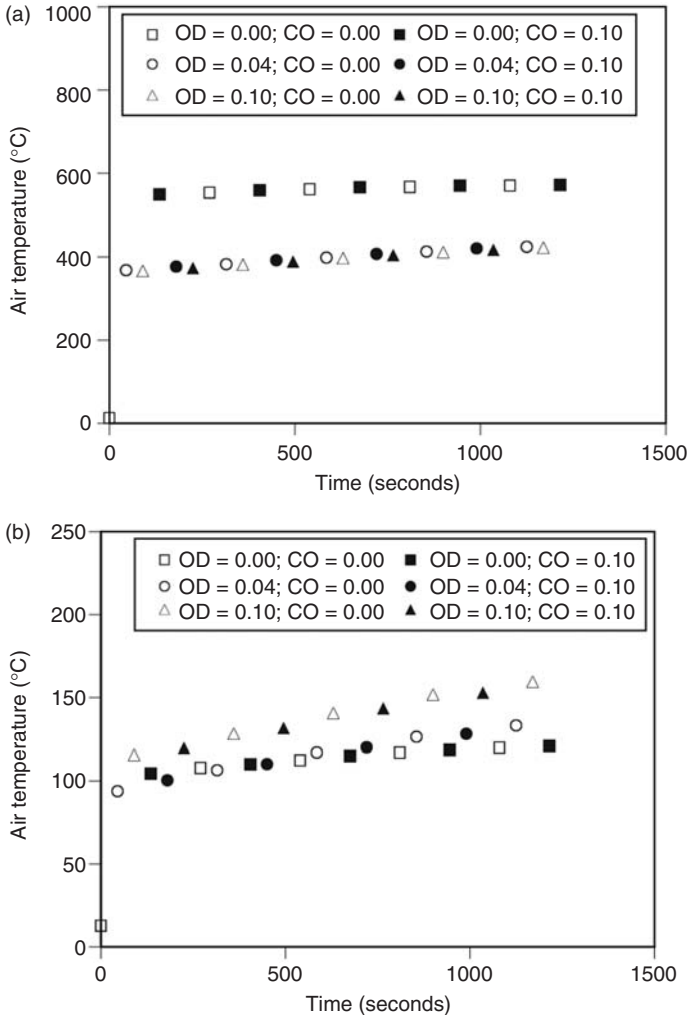


Figure 4. (a) Upper layer gas temperature dependence on OD and CO: upper layer gas temperatures are strongly dependent on the presence or absence of soot, controlled by the OD parameter. There is almost no dependence on the carbon monoxide concentration, which is determined by the value of the CO parameter; (b) Lower layer gas temperature dependence on OD and CO: lower layer gas temperature is dependent on both the CO and the OD parameters, but the effects of OD predominate.

Figure 4(b), the trend is the opposite of that noted above – temperature is directly related to OD. As shown in Figures 5(a) (upper wall), 5(b) (lower wall), 6(a) (ceiling), and 6(b) (floor), the temperature predictions for the four surfaces all follow the same general pattern – the temperatures are

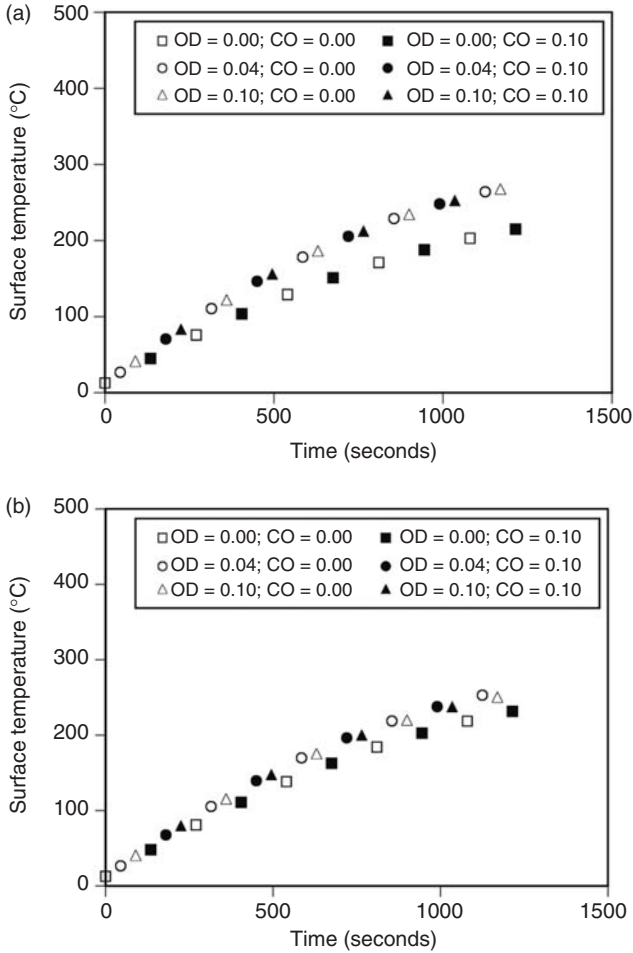


Figure 5. (a) Upper wall temperature dependence on OD and CO; (b) Lower wall temperature as a function of OD and CO.

noticeably lower in the soot-free cases than in the cases in which soot is present. For the ceiling and floor, the temperatures show a small direct dependence on the value of OD while upper and lower wall temperatures are essentially independent of the soot parameter, so long as it is nonzero.

The observed temperature trends are attributed to the effects of radiation transport. The upper gas layer is heated by mass transport via the fire plume and cooled by radiation. Conversely, radiation is the main heating mechanism for the lower layer and for the surfaces. In the absence of soot, upper layer emissivity is low and the layer does not readily lose energy.

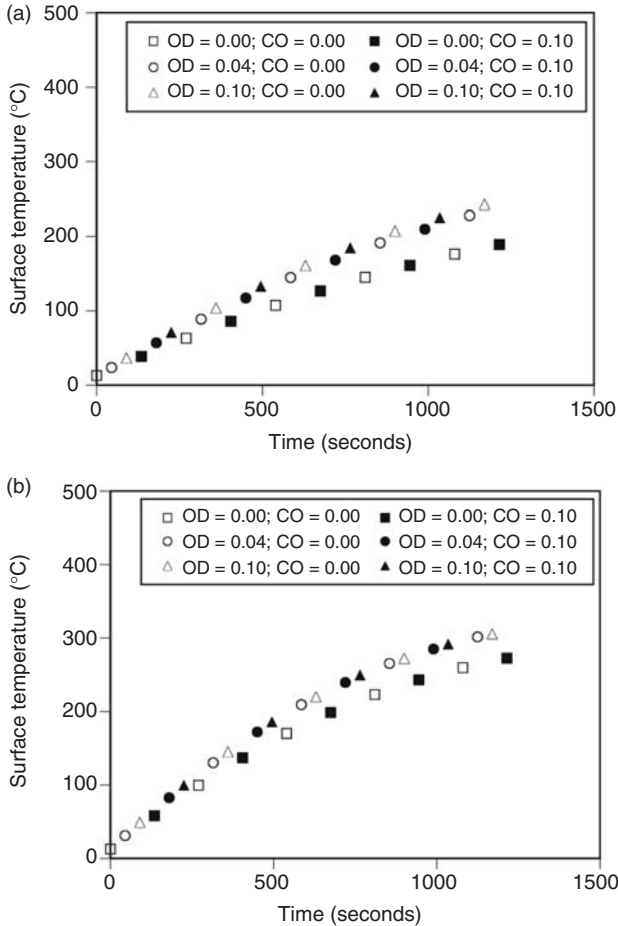


Figure 6. (a) Ceiling temperature dependence on OD and CO; (b) Floor temperature dependence on OD and CO.

If there is even a small amount of soot (OD is nonzero), then the upper layer emissivity is much higher and cooling is much more efficient. Surface temperatures exhibit the inverse behavior, becoming hotter as the radiation from the upper layer increases. The upper layer temperatures are nearly the same for all nonzero OD values and, since the surface absorptivities (as defined in the thermophysical database) are constants, the surface temperatures are also very similar. Because the lower layer gas absorptivity increases with increasing OD value while the source (upper layer) temperature is essentially constant, there is a significant direct temperature dependence on OD.

Changes in the CO input had negligible effects on the predicted gas and surface temperatures. In real fires, the production of carbon monoxide affects temperatures in two ways: first, by reducing the effective heat of combustion and, second, by changing the carbon dioxide and soot concentrations (which affect radiation transport among the gas layers and the various surfaces). CFAST does not include the direct effect on heat release rate but it does implicitly include the second.

The CO and OD parameters are specified independently, but their effects are coupled because both are specified as ratios with carbon dioxide. Thus, the mass balance condition enforced by CFAST requires that carbon that goes into carbon monoxide is unavailable for production of soot or carbon dioxide, both of which are parameters of the radiation transport algorithm [9]. Because this is a second order effect, the resulting temperature changes are very small and are barely noticeable.

The species concentration predictions are generally consistent with the above interpretation. For both the upper [Figure 7(a)] and lower [Figure 7(b)] layers, an increase in the production of carbon monoxide causes a reduction in the amount of soot. Likewise, carbon monoxide concentration has an inverse dependence on OD for both layers [Figure 8(a) and 8(b)], except for the case of zero soot in the lower layer. Finally, Figure 9(a) and 9(b) show that, for a given value of either the OD or CO input, carbon dioxide concentrations are inversely related to the other input, except in the absence of soot in the lower layer. When OD is zero in the lower layer, both carbon monoxide and carbon dioxide have lower than expected initial concentrations and the change in concentration over time does not follow the trends established for other values of OD.

COMPARISON WITH EXPERIMENTAL DATA

As shown above, the OD input has diminishing effects above a value of about 0.04. Therefore, a value of 0.06 was chosen as a reasonable estimate for the diesel fuel used in the Shadwell/688 tests. The CO parameter is not critical, except for prediction of the carbon monoxide concentration itself, so any reasonable value is acceptable. A value of 0.56 was selected this was the mean value measured by the gas analysis system over the test period. Predicted compartment air temperatures were compared with experimental values to evaluate the accuracy of the model.

In order to compare the model predictions with experiment, the CFAST-predicted interface height was chosen as the demarcation between the upper and lower layers. The use of estimated interface heights (based on thermocouple data) was considered, but it was believed that the comparison

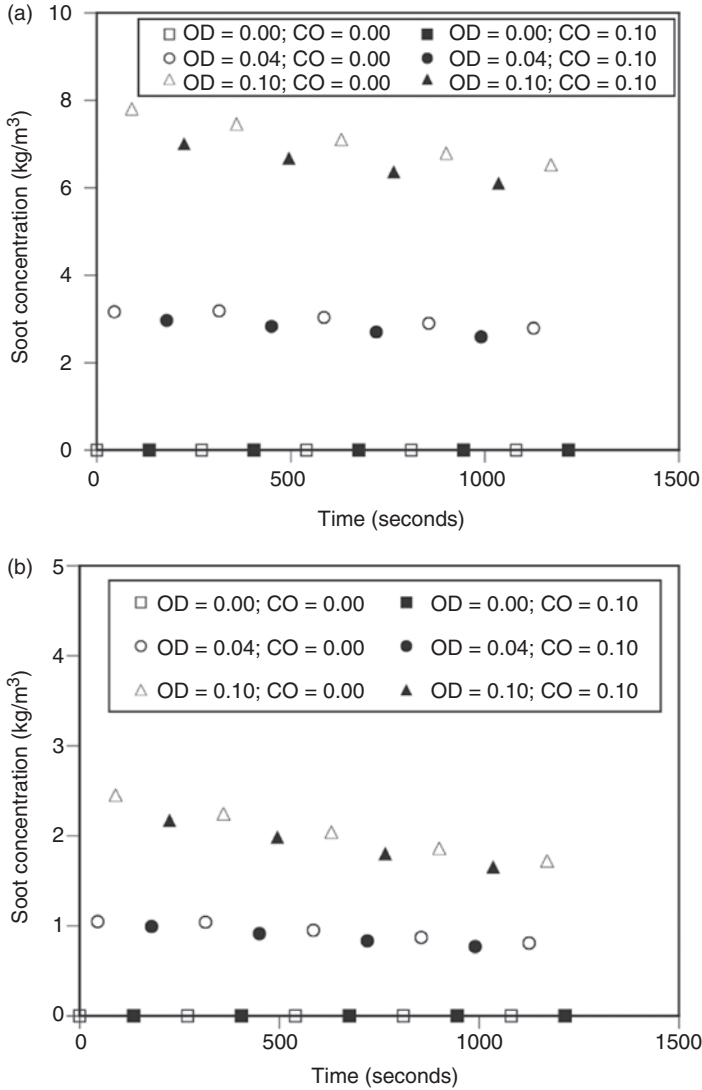


Figure 7. (a) Upper layer soot concentration dependence on OD and CO: upper layer soot concentrations increase approximately linearly with OD (compare different symbol shapes) and, as expected, decrease with increasing values of the CO parameter (compare solid versus open symbols); (b) Lower layer soot concentration dependence on OD and CO: soot concentrations in the lower layer follow the same pattern as seen in the upper but the absolute concentration values are lower, in keeping with the ‘cleaner’ nature of the lower layer.

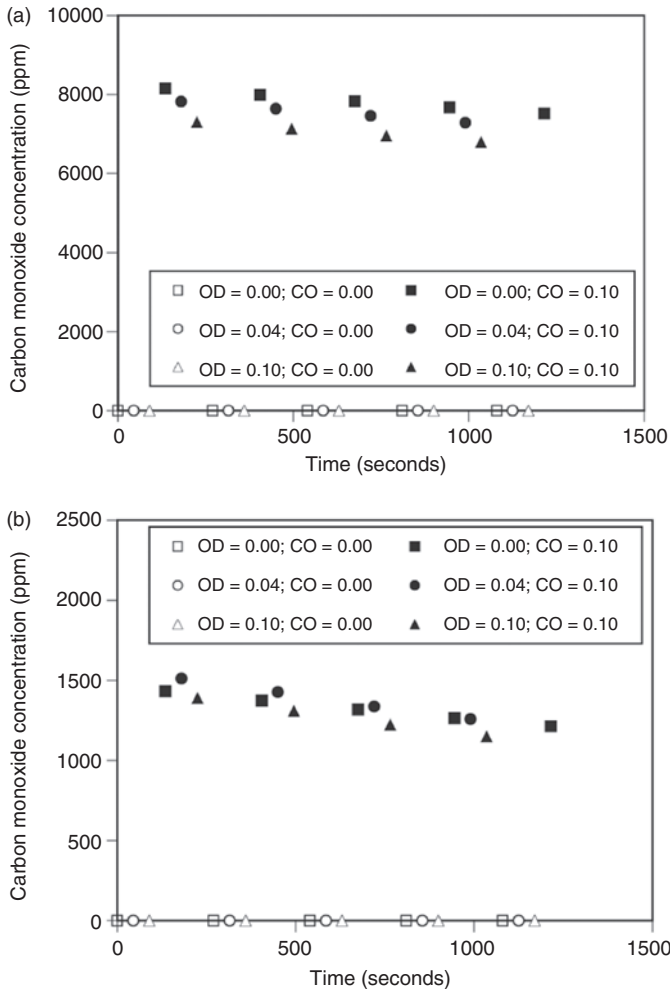


Figure 8. (a) Upper layer carbon monoxide concentration dependence on OD and CO: the behavior of carbon monoxide in the upper layer is inversely related to OD (compare different symbol shapes) except when the CO is set to zero, in which case the model completely suppresses the creation of carbon monoxide; (b) Lower layer carbon monoxide concentration dependence on OD and CO: in the lower layer, the carbon monoxide concentration follows the expected trend for nonzero values of the OD input but not when OD is zero (squares).

would be more meaningful if made between the temperatures that CFAST ‘thinks’ are in a given layer and the actual temperatures in that region.

Except for the first few seconds, while the interface was developing, the lower two thermocouples were below the interface and the remaining four

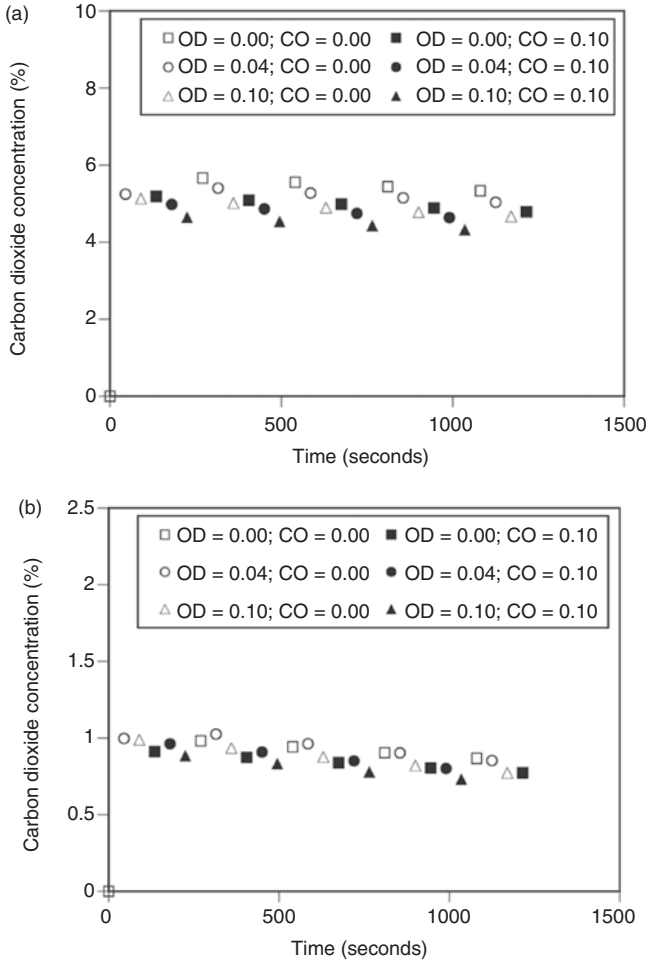


Figure 9. (a) Upper layer carbon dioxide concentration dependence on OD and CO: because carbon monoxide and soot are relatively minor constituents of the combustion products, even large percentage changes in their concentrations have small effects on the concentration of the dominant constituent, carbon dioxide; (b) Lower layer carbon dioxide concentration dependence on OD and CO: the behavior of carbon dioxide in the lower layer is qualitatively similar to that of carbon monoxide, with the OD equals zero cases (squares) behaving differently from the other cases.

were above. Mean temperatures and estimated standard deviations were calculated for each of these groups and plotted along with the model air temperature predictions in Figure 10. The values predicted by CFAST 6.0.7 are well within the experimental errors, except during the initial stages of the fire when the model consistently over predicts the temperatures.

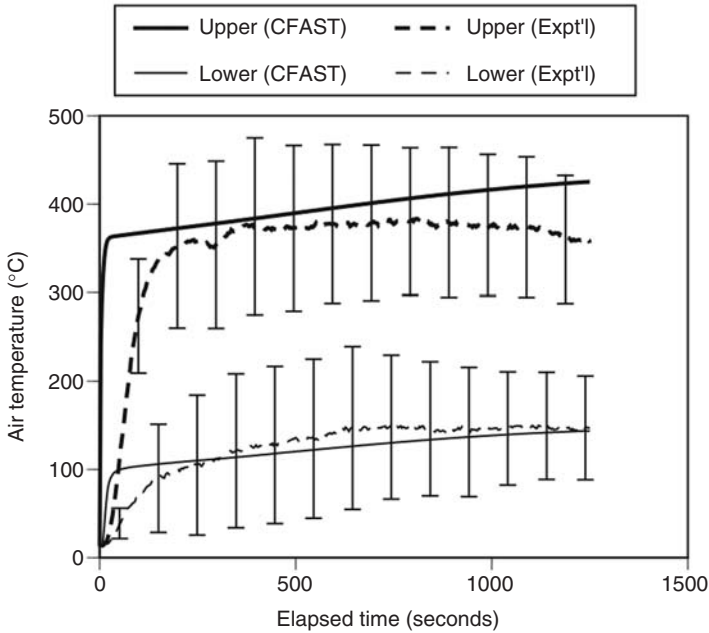


Figure 10. Experimental vs. predicted air temperatures: the experimental mean air temperatures and estimated population standard deviations are compared with the upper and lower layer gas temperature predictions from CFAST 6.0.7.

DISCUSSION OF MODEL PREDICTIONS

Sensitivity to CJET

CJET is expected to most strongly affect the ceiling temperatures during the first seconds of the simulation. To investigate the sensitivity of the predictions to this parameter, simulations were run with each of the four possible CJET values ('All,' 'Off,' 'Ceiling,' and 'Walls'). The values discussed in the previous section were used for all other model inputs. Ceiling temperature predictions, shown in Figure 11, were indistinguishable among the four cases.

Sensitivity to Radiative Fraction

Higher values for RF result in more energy radiated from the fire, leaving less to be convected into the upper layer. Therefore, it was anticipated that

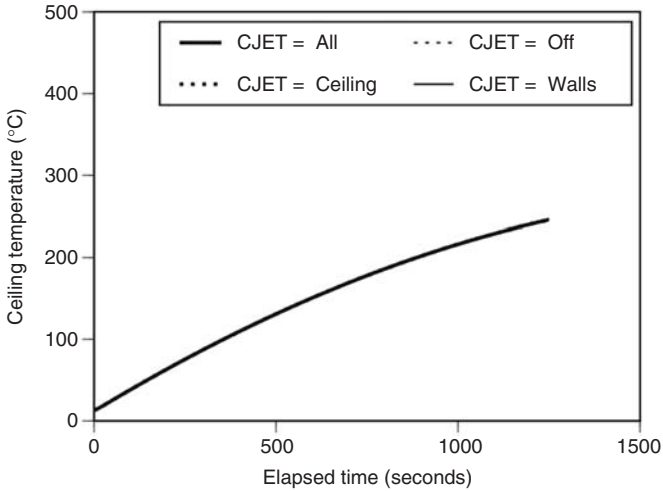


Figure 11. Effects of CJET on ceiling temperature: ceiling temperatures were independent of the value used for the CJET parameter.

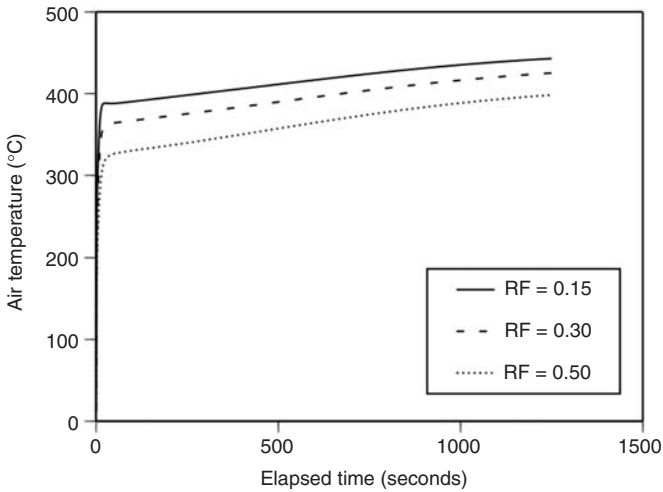


Figure 12. Upper layer gas temperature dependence on radiative fraction (RF): increasing values of RF reduce the energy available for convection to the upper layer, resulting in lower upper layer air temperatures.

the upper layer temperature would be inversely dependent on RF and this expectation proved to be correct, as shown in Figure 12.

It was also expected that species concentrations, which are controlled by the previously discussed CO and OD parameters, would not be affected by RF. However, it was found that soot, carbon monoxide and carbon

dioxide all are dependent on RF. Figure 13(a) illustrates this effect for the case of upper layer soot, where there is a direct dependence; the other species behave similarly. In the lower layer, the species are inversely related to RF [as shown, for soot, in Figure 13(b)].

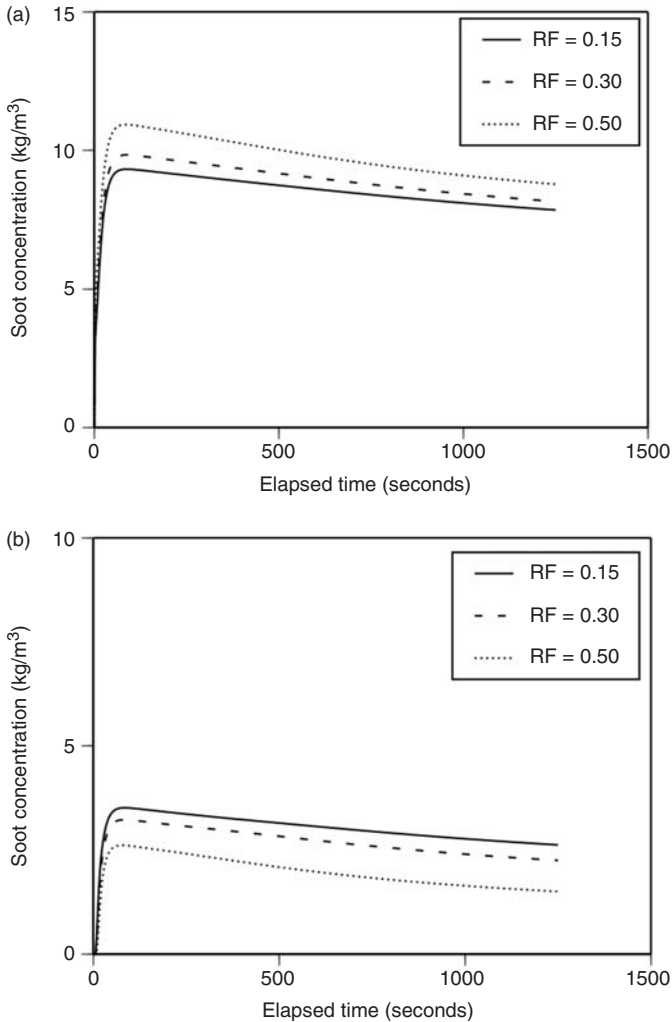


Figure 13. (a) Upper layer soot concentration dependence on radiative fraction (RF): increasing values of RF increase the soot concentrations for the upper layer. Similar effects are also seen for carbon monoxide and carbon dioxide concentrations; (b) Lower layer soot concentration dependence on RF: the lower layer trend is the opposite of that seen in the upper layer. This effect is also observed for carbon monoxide and carbon dioxide concentrations.

Anomalous Predictions

A number of anomalies in the CFAST 6.0.7 predictions were observed in this study. The odd behavior of the carbon monoxide [Figure 8(b)] and carbon dioxide [Figure 9(b)] predictions for the lower layer have already been mentioned. In these cases, the expected inverse correlation between species concentration and OD parameter is found in the OD range from 0.02 to 0.10 but breaks down when OD is zero.

Similarly, the lower layer air temperature [Figure 4(b)] behavior is qualitatively different when there is no soot, as compared to the cases in which there is soot. The no-soot temperatures during the early portion of the simulation were typical of those predicted for much higher OD inputs while they approached values expected for low OD inputs near the end of the simulation. The predicted air temperatures are higher than expected at the start of the simulation but, because the slope of the curve is relatively flat, they are close to the expected values by the end of the simulation.

Finally, note that the ceiling and floor temperatures do not behave as expected (Figure 14) – the ceiling is cooler than the walls and the floor is hotter. Consideration of the heat transfer mechanisms involved leads to the expectation that the ceiling should be hotter, assuming similar material properties for the floor and ceiling. In the case at hand, the thermo-physical properties for the ceiling and floor were identical. This temperature inversion

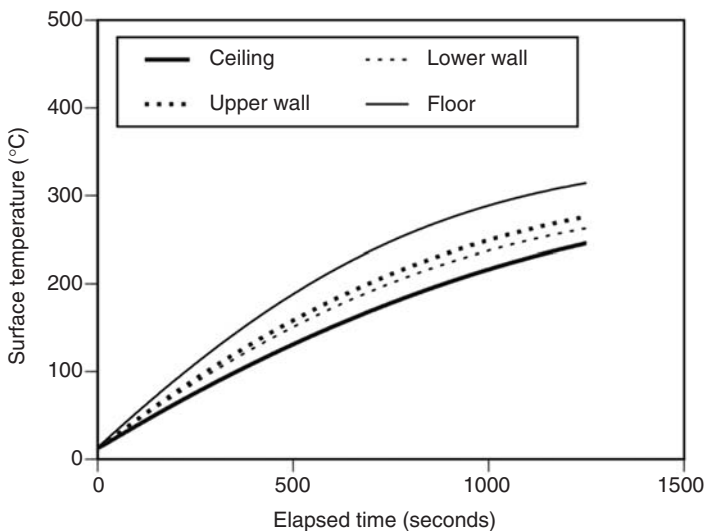


Figure 14. Predicted surface temperatures: the ceiling temperature is predicted by CFAST 6.0.7 to be lower than the wall temperatures while the floor temperature is higher.

was previously seen in CFAST 3.1.4, but not in version 2.1. Since most of these anomalies appear to be related to the OD parameter, it is believed that they may be due to interactions between the radiation transport algorithm [9] (which was introduced in version 3 and, for the first time, made use of the OD input parameter) and other heat and species transport software.

CONCLUSIONS

The feasibility of developing a CFAST fire specification, based almost entirely on literature values for fuel parameters and on physically reasonable approximations, has been demonstrated. It has also been shown that, using this specification, CFAST is capable of producing temperature predictions in very good agreement with experimental data for a shipboard fire scenario.

A sensitivity analysis has shown that the OD parameter plays a very important part in the prediction of gas temperatures, especially in the upper layer. OD also controls visibility and contributes to toxicity predictions both directly, through soot production, and indirectly, through its effects on oxygen, carbon dioxide and carbon monoxide concentrations. As a result, selecting a 'good' value for this parameter is critical for CFAST applications in which temperatures, soot concentration or visibility are important. This includes estimation of fire spread, habitability and egress times. In contrast, the choice of the CO parameter value is not critical, except for prediction of the carbon monoxide concentration itself.

In the event that accurate species predictions are required, then both OD and CO must be known, as functions of time, for the entire burning period. In practice, this knowledge is unlikely to be available and, for these cases, a field model may be a more appropriate tool. For 'clean' fuels (methanol, for example), an OD value close to zero is appropriate while, for the 'dirty' fires typical of many longer chain hydrocarbon fuels, a value near 0.06 is reasonable. It is probably best to select a nominal value, based on available information, and bracket that value with high and low extremes.

The choice of ceiling jet algorithm had no measurable effect on the predicted temperatures in the fire scenario. However, since it is expected that CJET might have an effect in cases in which there is a larger fire plume or a lower overhead, it is suggested that at least the 'Off' and 'Ceiling' cases be tested.

Radiative fraction has a significant effect on temperature predictions, as expected, but the species concentrations also have an unanticipated dependence on the RF input. Values of RF near zero or larger than about 0.5 typically caused convergence problems.

Several anomalous surface temperature predictions, which appear to be related to the improved radiation transport model, were also found. Both the RF-species and the anomalous surface temperature effects are thought to be due to unintended interactions between nominally independent portions of the CFAST software.

ACKNOWLEDGMENTS

The work described in this report was performed by the Chemistry Division of the Materials Science and Component Technology Directorate, Naval Research Laboratory. The work was funded by the Office of Naval Research, Code 334, under the Damage Control Task of the Surface Ship Hull, Mechanical, and Electrical Technology Program (PE0602121N). The author wishes to thank Jean Bailey (NRL Code 6183), for her assistance in performing the CFAST modeling, and Rick Peacock (NIST) for invaluable assistance in setting up the model inputs and interpreting the results.

REFERENCES

1. Peacock, R.D., Forney, G.P., Reneke, P., Portier, R. and Jones, W.W., "CFAST, the Consolidated Model of Fire Growth and Smoke Transport," Technical Note 1299, Gaithersburg, MD USA, National Institute of Standards and Technology, 1993.
2. Babrauskas, V. and Peacock, R.D., "Heat Release Rate: The Single Most Important Variable in Fire Hazard," *Fire Safety Journal*, Vol. 18, 1992, pp. 255–272.
3. Portier, R.W., Reneke, P.A., Jones, W.W. and Peacock, R.D., "A User's Guide for CFAST Version 1.6. NISTIR 4985, National Institute of Standards and Technology," Gaithersburg, MD, USA, 1992.
4. Collier, P.C.R., "Fire in a Residential Building: Comparisons between Experimental Data and a Fire Zone Model," *Fire Technology*, Vol. 32, 1996, pp. 195–218.
5. He, Yaping and Beck, Vaughan, "Smoke Spread Experiment in a Multi-storey Building and Computer Modeling," *Fire Safety Journal*, Vol. 28, 1997, pp. 139–164.
6. Rho, J.S. and Ryou, H.S., "A Numerical Study of Atrium Fires Using Deterministic Models," *Fire Safety Journal*, Vol. 33, 1999, pp. 213–229.
7. Hu, L.H., Li, Y.Z., Huo, R. and Wang, H.B., "Smoke Filling Simulation in a Boarding-Arrival Passage of an Airport Terminal Using Multicell Concept," *Journal of Fire Science*, Vol. 23, 2005, pp. 31–53.
8. Bailey, J.L., Forney, G.P., Tatem, P.A. and Jones, W.W., "Development of an Algorithm to Predict Vertical Heat Transfer through Ceiling/Floor Conduction," *Fire Technology*, Vol. 34, No. 2, 1998, pp. 139–155.
9. Hoover, J.B., Bailey, J.L. and Tatem, P.A., "An Improved Radiation Transport Submodel for CFAST," *Combustion Science and Technology*, Vol. 127, 1997, pp. 213–229.
10. Bailey, J.L., Forney, G.P., Tatem, P.A. and Jones, W.W., "Development and Validation of Corridor Flow Submodel for CFAST," *Journal of Fire Protection Engineering*, Vol. 12, 2002, pp. 139–161.

11. Hoover, J.B. and Tatem, P.A., "Application of CFAST to Shipboard Fire Modeling I: Development of the Fire Specification," Memo Report NRL/MR/6180-00-8466, Naval Research Laboratory, Washington, DC, USA, 2000.
12. Hoover, J.B., Tatem, P.A. and Williams, F.W., "Meta-Analysis of Data from the Submarine Ventilation Doctrine Test Program," Memo Report NRL/MR/6180-98-8168, Naval Research Laboratory, Washington, DC, USA, 1998.
13. Peacock, R.D., Jones, W.W., Reneke, P.A. and Forney, G.P., "CFAST — Consolidated Model of Fire Growth and Smoke Transport (Version 6) User's Guide, Special Publication 1041, National Institute of Standards and Technology," Gaithersburg, MD, USA, 2005.
14. Jones, W.W., Peacock, R.D., Forney, G.P. and Reneke, P., "CFAST — Consolidated Model of Fire Growth and Smoke Transport (Version 6) Technical Reference Guide, Special Publication 1026, National Institute of Standards and Technology," Gaithersburg, MD, USA, 2005.
15. Kanury, A.M., Introduction to Combustion Phenomena, Gordon and Breach, New York, NY, 1975, p. 144.
16. ASTM "Standard Specification for Diesel Fuel Oils", ASTM Specification D975-98a, Annual Book of ASTM Standards, Section 5, Petroleum Products, Lubricants and Fossil Fuels, West Conshohocken, PA, ASTM International, 1999, Vol. 05.01, p. 340.
17. Clarke, F.B., "Fire Hazards of Materials: An Overview," Fire Protection Handbook. 15th Ed., Quincy, MA, USA, National Fire Protection Association, 1981, Table 4-12A, pp. 4-120.
18. Naval Sea Systems Command, Military Specification: Fuel, Naval Distillate, MIL-F-16884J, Naval Sea Systems Command, Washington, DC, 1995, p. 6.
19. Handbook of Aviation Fuel Properties, 3rd Ed., Society of Automotive Engineers, Warrendale, PA, USA, 2004, Figure 2-16, pp. 2-21.
20. Purser, D.A., "Toxicity Assessment of Combustion Products", SFPE Handbook of Fire Protection Engineering. 1st Ed., Society of Fire Protection Engineers, Boston, MA, 1988, Table 1-14.7, pp. 1-222.